Vortex dynamics in the nonlinear Schrödinger equation

Michael J. Quist
Department of Physics, Cornell University, Ithaca, New York 14850
(Received 14 July 1998)

The dynamics of a two-dimensional vortex are analyzed within the framework of the nonlinear Schrödinger equation. Both a bare vortex and a vortex with an external mass trapped in a finite-sized core are considered. The bare vortex motion is found to be damped at all frequencies, while the finite core has a single resonant frequency. The force exerted by the fluid on the finite core can be expressed as a sum of dissipative and Magnus forces for sufficiently low frequencies, even when the core is small. [S0163-1829(99)03430-X]

I. INTRODUCTION

Vortices represent an important class of excitations in many-body systems. They are associated with quantized circulation and dissipative flow in superfluids,[1] flux penetration and the breakdown of superconductivity in type-II superconductors,[2] and the Kosterlitz-Thouless phase transition in two-dimensional systems.[3] The study of vortices in classical fluids is also well-developed. The aim of this paper is to address two questions pertaining to vortex dynamics in a two-dimensional boson fluid. First, we would like to determine whether there is an undamped or weakly damped mode with a moving vortex core; here the core velocity is measured relative to the fluid at infinity. Second, we want to understand the dynamics of the core when an external mass is trapped in it. A commonly-used phenomenological model expresses the force on a moving vortex core as the sum of a damping force acting parallel to the core velocity (again, relative to distant fluid) and a Magnus force acting perpendicular to it.[4] This type of model can describe classical vortex dynamics; it is also experimentally known to be valid in superfluid ^{4}He, at least when the core is a macroscopic object.[5] We would like to know whether such a model also describes the dynamics at shorter length scales, on the order of the size of a bare vortex core. We work within the nonlinear Schrödinger approximation, which is applicable in the limit of a dilute, weakly interacting Bose gas. A recent publication by Demircan, Ao, and Niu addressed similar questions within this framework;[6] we found that this work contained several mathematical errors invalidating its main results.

The outline of our paper is as follows. We first present the basic vortex model and derive equations of motion for the core and the phonon modes to which it couples. We then show how these equations can be modified to include a massive object in the core. Next we discuss the qualitative features of the normal modes of the system and use numerical methods to find them. Finally we present our results and conclusions.

II. VORTEX MODEL

We start with the following Lagrangian,[7] which describes a two-dimensional system of bosons interacting via a delta-function pseudopotential:

$$L=\int d^2r\left\{ i\hbar\Psi^*\dot{\Psi}-\frac{\hbar^2}{2m}|\nabla\Psi|^2+\mu|\Psi|^2-\frac{\lambda}{2}|\Psi|^4\right\}. \tag{1}$$

Here m is the boson mass, μ the chemical potential, and λ the interaction strength. This can be put in dimensionless form by a rescaling of variables. We let $\Psi\rightarrow(\mu/\lambda)^{1/2}\Psi$, $\mathbf{r}\rightarrow(\hbar^2/m\mu)^{1/2}\mathbf{r}$, and $t\rightarrow(\hbar/\mu)t$ to obtain

$$L=\frac{\hbar^2\mu}{m\lambda}\int d^2r\left\{ i\Psi^*\dot{\Psi}-\frac{1}{2}|\nabla\Psi|^2+|\Psi|^2-\frac{1}{2}|\Psi|^4\right\}. \tag{2}$$

The prefactor is irrelevant for the present (classical) analysis, since the classical equations of motion are invariant under a rescaling of L. However, note that the action $\int L\,dt$ acquires a prefactor of $\hbar^3/m\lambda$, which is much larger than $\hbar$ provided that $\lambda\ll\hbar^2/m$; this defines the weakly interacting limit. In this limit the correspondence principle applies, at least naively, and quantum fluctuations around the classical behavior are expected to be small. The Euler-Lagrange equation for the complex field $\Psi(\mathbf{r},t)$ is

$$i\dot{\Psi}=-\frac{1}{2}\nabla^2\Psi+(|\Psi|^2-1)\Psi. \tag{3}$$

This is the well-known nonlinear Schrödinger equation, derived for the imperfect Bose gas by Gross and Pitaevskii.[8,9] It has since been applied to vortex lines in superfluids by a number of authors (see, e.g., Refs. 10–12). It can be given a hydrodynamic interpretation by making the Madelung transformation $\Psi=\sqrt{\rho}e^{i\phi}$, where ρ and ϕ are the fluid density and velocity potential ($\mathbf{v}=\nabla\phi$) respectively. The equations of motion for these variables are

$$\frac{\partial\rho}{\partial t}=-\nabla\cdot(\rho\mathbf{v}), \tag{4a}$$

$$\frac{d}{dt}(\rho\mathbf{v})=\nabla\cdot\boldsymbol{\sigma}, \tag{4b}$$

where $d/dt\equiv\partial/\partial t+\mathbf{v}\cdot\nabla$ is the convective derivative and the components of the stress tensor $\boldsymbol{\sigma}$ are

$$\sigma_{ij}=-\frac{1}{2}(\rho^2-1)\,\delta_{ij}+\frac{1}{4}\left(\partial_i\partial_j\rho-\frac{1}{\rho}(\partial_i\rho)(\partial_j\rho)\right). \tag{5}$$

Except for the derivative terms in the stress tensor, these are the equations of motion for an ideal classical fluid with pressure $p=\frac{1}{2}(\rho^2-1)$.

Equation (3) has time-independent vortex solutions of the form $f(r)e^{in\theta}$ for any integer n. We consider only $n=1$, in which case the solution is

$$\Psi_0(\mathbf{r})=f(r)e^{i\theta}, \tag{6}$$

where $f(r)$ satisfies

$$f''(r)+\frac{1}{r}f'(r)+\left(2-2f(r)^2-\frac{1}{r^2}\right)f(r)=0. \tag{7}$$

The asymptotic behaviors of the solution for large and small r can be expressed as power series:

$$f(r)\sim\begin{cases} A\,r-\dfrac{A}{4}r^3+\left(\dfrac{A}{48}+\dfrac{A^3}{12}\right)r^5+\cdots & \text{as } r\to 0, \\ 1-\dfrac{1}{4\,r^2}-\dfrac{9}{32\,r^4}-\cdots & \text{as } r\to\infty. \end{cases} \tag{8}$$

The value of $A\equiv f'(0)$ is not determined by the asymptotics and must be found numerically. We used a shooting method and found $A\simeq 0.825$, which does not agree with the value of $\sqrt{2}$ given in Ref. 6, but does agree with the numerical work of Kawatra and Pathria.[12]

In order to investigate vortex motion, we consider perturbations around a single-vortex solution with a moving core. The new dynamical variables are defined by

$$\Psi(\mathbf{r},t)=\Psi_0(\mathbf{r}-\mathbf{r}_0(t))+\delta\Psi(\mathbf{r}-\mathbf{r}_0(t),t), \tag{9}$$

where $\mathbf{r}_0(t)$ is the location of the vortex core. Changing variables in Eq. (3) and linearizing in $\delta\Psi$ and $\dot{\mathbf{r}}_0$ gives

$$i\,\delta\dot{\Psi}=i\dot{\mathbf{r}}_0\cdot\boldsymbol{\nabla}\Psi_0-\frac{1}{2}\nabla^2\delta\Psi+(2|\Psi_0|^2-1)\,\delta\Psi+(\Psi_0)^2\delta\Psi^*. \tag{10}$$

At this point we decompose $\delta\Psi$ into cylindrical harmonics: $\delta\Psi(\mathbf{r})=\Sigma_m\delta\Psi_m(r)e^{im\theta}$. It is also convenient to represent $\mathbf{r}_0$ by a complex number $r_+\equiv\mathbf{r}_0\cdot(\hat{\mathbf{x}}+i\hat{\mathbf{y}})$. In Eq. (10), only the $m=0$ and $m=2$ modes couple to the dynamics of $\mathbf{r}_0$. The other modes can be set to zero, and the evolution of the relevant modes is given by

$$i\,\delta\dot{\Psi}_0=-\frac{1}{2}\,\delta\Psi_0''-\frac{1}{2r}\,\delta\Psi_0'+(2f^2-1)\,\delta\Psi_0+f^2\delta\Psi_2^*+\frac{1}{2}i\dot{r}_+\left(f'+\frac{f}{r}\right), \tag{11a}$$

$$-i\,\delta\dot{\Psi}_2^*=-\frac{1}{2}(\delta\Psi_2^*)''-\frac{1}{2r}(\delta\Psi_2^*)'+\left(2f^2-1+\frac{2}{r^2}\right)\delta\Psi_2^*+f^2\delta\Psi_0-\frac{1}{2}i\dot{r}_+\left(f'-\frac{f}{r}\right), \tag{11b}$$

where the primes represent differentiation with respect to r. We impose the constraint $\delta\Psi(\mathbf{0},t)=0$, so that $\mathbf{r}_0$ marks the true location of the vortex core. These equations then determine the motion of both the fluid and the core. In particular, since the $\delta\Psi_m$ and their time derivatives vanish as $r\to 0$, Eq. (11a) implies that

$$\dot{r}_+=-\frac{i\,\delta\Psi_0''(0)}{f'(0)}. \tag{12}$$

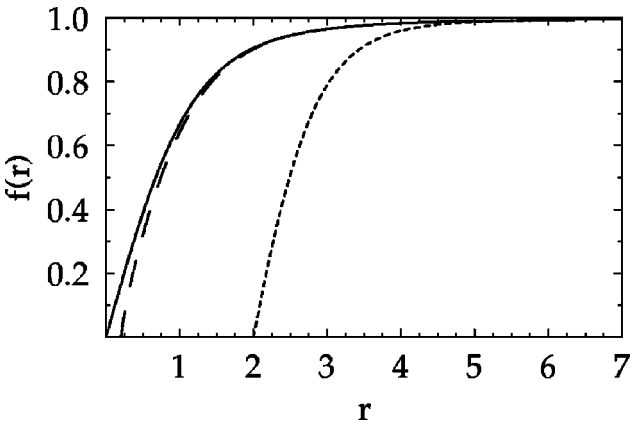

FIG. 1. Square root of the fluid density for the bare core (solid curve), small core (dashed curve), and large core (dotted curve).

III. FINITE CORE

We also would like to introduce an additional mass M, coupled to an arbitrary external force $\mathbf{F}(t)$ and confined to the center of the vortex. The question arises as to how this mass (which might physically represent a foreign particle trapped in the core) should interact with the fluid. We considered using a point mass constrained to lie at the vortex core, but found this model to be internally inconsistent for the following reason. If the perturbation $\delta\Psi$ is bounded, as the validity of our linearized approach requires, the fluid exerts no force on a point mass. (This is justified in the next paragraph.) The equation of motion for a point mass is therefore $M\ddot{\mathbf{r}}_0=\mathbf{F}$. On the other hand, for the mass to remain at the vortex core, Eq. (12) needs to be satisfied as well. The two equations for $\mathbf{r}_0$ cannot be satisfied simultaneously for arbitrary $\mathbf{F}$, so the model is ill-defined. Instead, we will treat the core as a hard disk of finite radius a. This is a simple approximation to a more realistic interaction between the fluid and a trapped particle, such as a Lennard-Jones potential. The fluid density must vanish inside the core, so the stationary vortex solutions now satisfy $f(a)=0$, and $\delta\Psi(\mathbf{r},t)=0$ for $r=a$. Figure 1 shows $f(r)$ for the three cases we considered: the bare core, a small core ($a=0.2$), and a large core ($a=2.0$). The time dependence of small perturbations in the fluid is still given by Eqs. (11a) and (11b).

For momentum to be locally conserved, the force on the core due to the fluid must equal the momentum crossing the boundary line $r=a$ per unit time. This condition can be expressed in terms of the stress tensor:

$$\frac{d\mathbf{F}^{\text{fluid}}}{ds}=\boldsymbol{\sigma}\cdot\hat{\mathbf{n}}, \tag{13}$$

where $\hat{\mathbf{n}}$ is the boundary's outward unit normal and ds is the line element along the boundary. Integrating this expression around the circumference of the core and using the form of the stress tensor given in Eq. (5), the force exerted on the mass by the fluid is found to be

$$F_+^{\text{fluid}} \equiv \mathbf{F}^{\text{fluid}} \cdot (\hat{\mathbf{x}} + i\hat{\mathbf{y}}) = \pi a f'(a)(\delta\Psi_0'(a) + (\delta\Psi_2^*)'(a)). \tag{14}$$

Note that as $a \to 0$, this force vanishes unless $\delta\Psi_0 + \delta\Psi_2^*$ diverges at least logarithmically, as asserted above. Here we mention that Ref. 6 draws its conclusions from the point-mass model, which we have argued to be inconsistent. Their presentation of this model differs from ours in that they introduce a mass term directly into the Lagrangian. This hides the inconsistency but does not remove it: it leads to a seemingly nontrivial equation of motion for $\mathbf{r}_0$ which is actually equivalent to $M\ddot{\mathbf{r}}_0 = \mathbf{0}$. A subsequent error (in joining inner and outer asymptotic solutions) disguises this equivalence, enabling the derivation of quantitative results that are essentially unsupported.

The equation of motion for the core mass is now

$$M\ddot{r}_+ = F_+^{\text{fluid}} + F_+, \tag{15}$$

where the external force has been written as a complex number $F_+ \equiv \mathbf{F} \cdot (\hat{\mathbf{x}} + i\hat{\mathbf{y}})$. Since the equations of motion [Eqs. (11a) and (11b) and (15)] are linear in F_+, r_+, $\delta\Psi_0$, and $\delta\Psi_2^*$, we will seek solutions in which all of these variables are proportional to $e^{i\omega t}$. The general solution can be then expressed as a sum over normal modes in the usual way.

IV. NORMAL MODES

For a finite core, the mode equations for frequency ω are

$$-M\omega^2 r_+ - \pi a f'(a)(\delta\Psi_0'(a) + (\delta\Psi_2^*)'(a)) = F_+, \tag{16a}$$

$$\delta\Psi_0'' + \frac{1}{r}\delta\Psi_0' + (2 - 4f^2 - 2\omega)\delta\Psi_0 - 2f^2\delta\Psi_2^* = -\omega r_+ \left(f' + \frac{f}{r}\right), \tag{16b}$$

$$(\delta\Psi_2^*)'' + \frac{1}{r}(\delta\Psi_2^*)' + \left(2 - 4f^2 - \frac{4}{r^2} + 2\omega\right)\delta\Psi_2^* - 2f^2\delta\Psi_0 = \omega r_+ \left(f' - \frac{f}{r}\right); \tag{16c}$$

the bare core will be considered as a special case with $a = M = F_+ = 0$. Equations (16b) and (16c) are coupled inhomogeneous linear ODEs for $\delta\Psi_0(r)$ and $\delta\Psi_2^*(r)$ which must be solved subject to homogeneous boundary conditions: the $\delta\Psi_m$ must remain finite as $r \to \infty$, and must vanish as $r \to a$. The most general solution will have the form of a particular solution to the inhomogeneous equations plus a linear combination of solutions to the corresponding homogeneous equations (obtained by setting $r_+ = 0$).

We now consider the solutions to the homogeneous equations. Given the order of the equations, there must be four such solutions. As $r \to 0$ their asymptotic behaviors are as follows: (a) $\delta\Psi_0 \sim r^6$ and $\delta\Psi_2^* \sim \text{const} \times r^2$; (b) $\delta\Psi_0 \sim 1$ and $\delta\Psi_2^* \sim \text{const} \times r^4$; (c) $\delta\Psi_0 \sim \ln r$ and $\delta\Psi_2^* \sim \text{const} \times r^4 \ln r$; and (d) $\delta\Psi_0 \sim r^2$ and $\delta\Psi_2^* \sim \text{const} \times 1/r^2$. In the opposite limit, as $r \to \infty$, two solutions are oscillatory, representing incoming and outgoing waves, one solution decays exponentially, and one solution grows exponentially. (The asymptotic solutions were found by Fetter.[10]) All other points ($r \neq 0$ or ∞) are regular points of Eqs. (16b) and (16c), so the $\delta\Psi_m$ and their derivatives can be specified freely.

In the case of the bare core, only inner solution (a) conforms to the boundary condition at the origin. If this function is followed to infinity, it will decompose into a linear combination of the four outer solutions, and in general (for arbitrary ω) the coefficient of the exponentially growing solution will not vanish. In other words, if the inner boundary condition is satisfied then the outer one will not be. Therefore, with a bare core there is no nonzero solution to the homogeneous equations, and the solution to the inhomogeneous equations will be unique and proportional to r_+.

In the case of a finite core, two linearly independent solutions satisfy the boundary condition at $r = a$, since $\delta\Psi_0'(a)$ and $(\delta\Psi_2^*)'(a)$ are independent free parameters. Both have some coefficient of overlap with the growing solution, so a linear combination can be formed for which the overlap is zero and both boundary conditions are satisfied. The general solution to the inhomogeneous equations is in this case the sum of a term proportional to r_+ and a term proportional to another free parameter. Physically we expect to find a unique solution where the mass is driven solely by the external force and the fluid contains only outgoing waves. This solution should be proportional to r_+. The free parameter associated with the homogeneous solution can be taken to be the amplitude of incoming waves. Once the solutions are found, the force exerted on the moving mass by the fluid is given by Eq. (14). At this point we resort to numerical techniques to determine the solutions for the two cases.

V. NUMERICAL METHODS AND RESULTS

No single numerical technique proved capable of solving Eqs. (16b) and (16c) over the entire range $a < r < \infty$. Instead, a different method was used for each of three regions: $a < r < a + 4$, $a + 4 < r \lesssim 2\pi/\omega$, and $2\pi/\omega \lesssim r < \infty$. In each region we found a single solution to the inhomogeneous equations and all four linearly independent solutions to the homogeneous equations. We then chose the appropriate coefficients for the homogeneous terms so that $\delta\Psi_0$ and $\delta\Psi_2^*$ satisfied the boundary conditions and joined smoothly at the boundaries between regions.

For the innermost region we used direct numerical integration, starting at $r = a$, to determine the homogeneous solutions. Because of the exponentially growing solution, the integration is unstable and loses precision with increasing r. We cut off the integration at $r = a + 4$; the exact placement was somewhat arbitrary, but it cannot be much further from the core. For the outermost region we used an asymptotic analysis. All the outer solutions to the homogeneous equations have asymptotic expansions of the form

$$\delta\Psi_0 \sim \frac{e^{kr}}{\sqrt{r}} \sum_{n=0}^{\infty} a_n(k) r^{-n}, \quad \delta\Psi_2^* \sim \frac{e^{kr}}{\sqrt{r}} \sum_{n=0}^{\infty} b_n(k) r^{-n}, \tag{17}$$

where k takes on one of the four values $\pm\sqrt{2\pm 2\sqrt{1+\omega^2}}$. Using the full outer asymptotic series for $f(r)$, the first few terms of which are shown in Eq. (8), the coefficients $a_n(k)$ and $b_n(k)$ can be found for arbitrarily large n. However, we found a_1/a_0 and b_1/b_0 to be of order $1/\omega$ for small ω, indicating that the $n=0$ terms in the series dominate for $r \gg 1/\omega$. We therefore kept only the $n=0$ terms and cut off the outermost region at $r \simeq 2\pi/\omega$. For the middle region we put Eqs. (16b) and (16c) on a grid, discretizing the derivatives in the most straightforward way. For small values of ω this middle region becomes quite large, so the average grid spacing needs to be reasonably large as well, to limit the number of grid points. On the other hand, the solutions still vary rapidly near the boundary at $r=a+4$, so the spacing must be much smaller there. A nonuniform grid was used to address both these problems.

Finally, note that an exact solution to the inhomogeneous equations, for all three regions, is

$$\delta\Psi_0 = \frac{1}{2} r_+ \left(f' + \frac{f}{r} \right), \quad \delta\Psi_2^* = \frac{1}{2} r_+ \left(f' - \frac{f}{r} \right). \tag{18}$$

This solution has a straightforward physical interpretation: it describes a stationary vortex centered at the origin. To see this, we can refer back to Eq. (9), the defining equation for $\delta\Psi$. A stationary vortex is described by $\Psi(\mathbf{r}, t) = \Psi_0(\mathbf{r})$, so

$$\delta\Psi(\mathbf{r} - \mathbf{r}_0(t), t) = \Psi_0(\mathbf{r}) - \Psi_0(\mathbf{r} - \mathbf{r}_0(t)) = \mathbf{r}_0(t) \cdot \boldsymbol{\nabla} \Psi_0(\mathbf{r}) \tag{19}$$

to first order in $\mathbf{r}_0$, and the angular components of this function are indeed given by Eq. (18).

We found that our procedure gave good results for a wide range of frequencies. The results were extremely insensitive to adjustment of the region boundaries, increased precision in the numerical integration, and the inclusion of more terms in the asymptotic expansions. Changing the number and spacing of grid points in the middle region, however, did cause small variations in the final results. In particular, for $10^{-3} \lesssim |\omega| \lesssim 5$ we estimate our errors to be on the order of a few percent.

First we analyzed elastic scattering. When incoming waves of unit power are scattered by a free core ($F_+ = 0$), the core responds with circular motion of a particular amplitude. Figure 2 shows the amplitude of response as a function of frequency for the bare, small, and large cores. Note that for a finite core the response depends on the mass; we show the results for $M=0$ only, but using $M>0$ causes no qualitative changes. A divergent response is seen only as $\omega \to 0$. The response functions for the small and large cores each have a single zero. These correspond to resonances in which the driven motion (discussed below) is undamped and the core motion is decoupled from the phonon field. The response function for the bare core, in contrast, is everywhere nonzero; we conclude that there is no undamped or weakly damped finite-frequency mode.

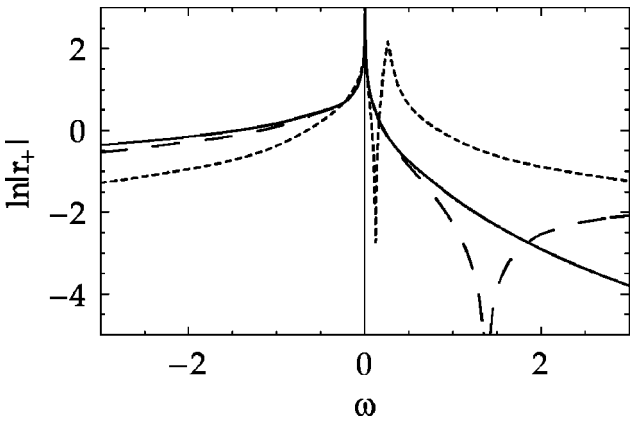

FIG. 2. Amplitude of circular motion in response to incoming waves of unit power and frequency ω. Results are for the bare core (solid curve), small core (dashed curve), and large core (dotted curve). $\ln|r_+|$ is shown.

For the small and large cores, we also analyzed driven motion. When a finite core is driven by the external force with unit speed, power is radiated as outgoing waves. The power is equal to that put into the system by the component of $\mathbf{F}$ parallel to the velocity: for $r_+ = 1/|\omega|$, corresponding to circular motion with unit speed, it is given by $P = \mathbf{F} \cdot \dot{\mathbf{r}}_0 = \pm \operatorname{Im} F_+$, where the sign is $+/-$ for positive/negative frequencies. This quantity is shown in Fig. 3 as a function of frequency. It is independent of M, and so provides a better measure of damping than the elastic scattering response. For the small core, the radiated power vanishes at $\omega \simeq 1.5$. At this frequency there are neither incoming nor outgoing waves; the perturbation is localized and dies off exponentially with increasing r. There is a similar resonance for the large core at $\omega \simeq 0.13$. For both cores, the motion is undamped as $\omega \to 0$. Results for other core sizes (not shown) suggest that these features are general: there is always a single positive-frequency resonance, the frequency of which varies inversely with a, and the damping always approaches zero for low frequencies.

Figure 4 shows the component of the force exerted by the fluid on the mass in the $-\dot{\mathbf{r}}_0 \times \hat{\mathbf{z}}$ direction. If the only contributor were the Magnus force,

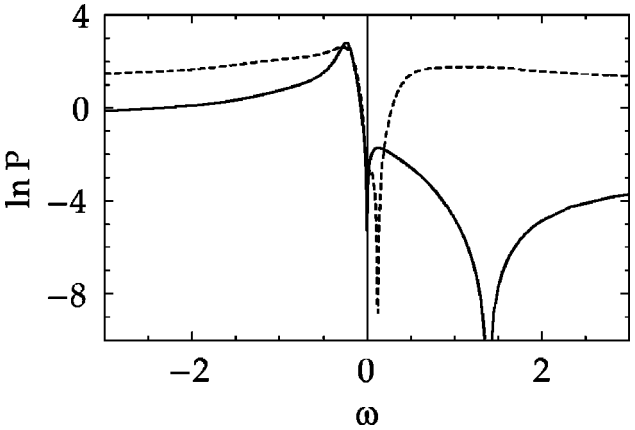

FIG. 3. Power dissipated by the small core (solid curve) and large core (dotted curve) in driven circular motion with unit speed and frequency ω. $\ln P$ is shown.

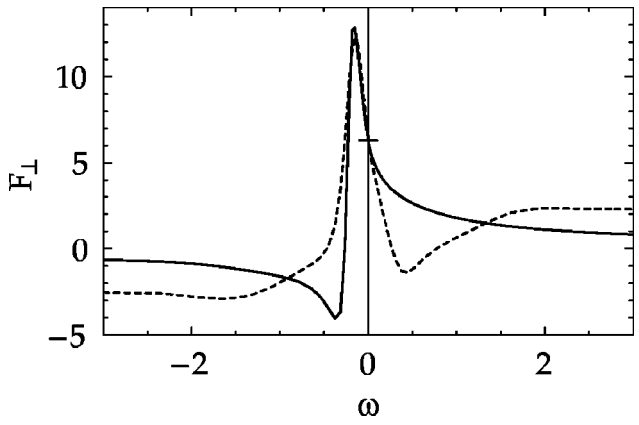

FIG. 4. Force in the $-\dot{\mathbf{r}}_0\times\hat{\mathbf{z}}$ direction exerted by the fluid on the small core (solid curve) and large core (dotted curve) in driven circular motion with unit speed and frequency ω. The mark on the vertical axis corresponds to $F_\perp = 2\pi$.

$$\mathbf{F}^{\text{Magnus}} = -2\pi\dot{\mathbf{r}}_0\times\hat{\mathbf{z}}, \tag{20}$$

this component would be identically 2π, which is marked on the vertical axis. Because we are driving the core with unit speed, the dependence on ω should vanish. Instead we see that the Magnus effect dominates only in the limit as $\omega\to 0$; for $|\omega|\gtrsim 1/10$, it can no longer account for the perpendicular component of the force.

VI. CONCLUSIONS

From our data we can answer both of our original questions. First, there is no undamped mode associated with the motion of a bare vortex. Second, the Magnus effect plays an important role in the dynamics of a finite core for the frequency range $|\omega|\lesssim 1/10$, even when the core is small. The Magnus force has been shown to be a general consequence of vortex motion in the adiabatic phase approximation.[13] We point out that this approximation is not valid when applied to the nonlinear Schrödinger equation, at least for an infinite system. To see why it must fail, again consider the solutions to Eqs. (16b) and (16c) in the limit as $r\to\infty$. The particular solution given by Eq. (18), as already stated, corresponds to a *stationary* vortex. The phase field of distant fluid does not follow the instantaneous location of the vortex, as it does within the adiabatic phase approximation, but rather maintains a fixed center. The most general solution to the mode equations has the same property, as the solutions to the corresponding homogeneous equations are either oscillatory or exponentially decaying, as discussed in Sec. IV, and cannot cancel this power-law behavior. The failure of the adiabatic phase approximation is also expected on physical grounds: since the low-frequency phonons travel with finite speed (the speed of sound $c=1$ in our units), the fluid cannot respond to low-frequency disturbances at a distance d in a time shorter than $1/d$. For this response time to be shorter than the time scale associated with the disturbance, we must have $d \ll 1/\omega$; at larger distances the phase of the fluid can no longer follow the core. Nevertheless we recover the Magnus effect for low frequencies, in agreement with results dependent on the adiabatic phase approximation, suggesting that the discrepancy at large distances is not crucial. For high frequencies, the Magnus force ceases to play a role. Note that this transition occurs while the phonon wavelength is still very large compared to the size of the core: for $\omega = 1/10$, the phonon wavelength is around 60. For superfluid ^{4}He, the transition frequency is 20–30 GHz, corresponding to a phonon wavelength of 100 Å.

ACKNOWLEDGMENT

This work was performed with the kind support of Cornell University.

[1] R. P. Feynman, in *Progress in Low Temperature Physics*, edited by C. J. Gorter (North-Holland, Amsterdam, 1955), Vol. 1.
[2] M. Tinkham, *Introduction to Superconductivity* (McGraw Hill, New York, 1996).
[3] J. M. Kosterlitz and D. J. Thouless, J. Phys. C **6**, 1181 (1973).
[4] R. J. Donnelly, *Quantized Vortices in Helium II* (Cambridge University Press, Cambridge, England, 1991), Chap. 3.
[5] W. F. Vinen, Proc. R. Soc. London, Ser. A **260**, 218 (1961).
[6] E. Demircan, P. Ao, and Q. Niu, Phys. Rev. B **54**, 10 027 (1996).
[7] J. W. Negele and H. Orland, *Quantum Many-Particle Systems* (Addison-Wesley, Reading, MA, 1987).
[8] E. P. Gross, Nuovo Cimento **20**, 454 (1961).
[9] L. P. Pitaevskii, Zh. Éksp. Teor. Fiz. **40**, 640 (1961) [Sov. Phys. JETP **13**, 451 (1961)].
[10] A. L. Fetter, Phys. Rev. **138**, A709 (1965).
[11] A. L. Fetter, Phys. Rev. **138**, A429 (1965).
[12] M. P. Kawatra and R. K. Pathria, Phys. Rev. **151**, 132 (1966).
[13] P. Ao and D. J. Thouless, Phys. Rev. Lett. **70**, 2158 (1993).